Magnetization reversal mechanism in $La_{0.67}Sr_{0.33}MnO_3$ thin films on $NdGaO_3$ substrates

M. Mathews, E. P. Houwman,[a] H. Boschker, G. Rijnders, and D. H. A. Blank
MESA+ Institute for Nanotechnology, University of Twente, 7500 AE Enschede, The Netherlands

(Received 2 September 2009; accepted 13 November 2009; published online 5 January 2010)

The field angle dependence of the coercive field of $La_{0.67}Sr_{0.33}MnO_3$ thin films grown epitaxially on $NdGaO_3$ substrates with different crystallographic orientations was determined. All films show uniaxial anisotropy. The angle dependence of the coercivity is best described by a two-phase model, explaining the strong increase in the coercive field for increasing field angles, away from the easy axis direction, as well as the sharp decrease for angles close to the hard direction. This implies that magnetization reversal starts with the depinning of domain walls, analogous to the Kondorsky model. With increasing field the reversal in the domains is not abrupt, but is determined by the gradual displacement of the domain walls. These results are of significance for understanding and possibly engineering of the switching behavior of magnetic tunnel junctions. © *2010 American Institute of Physics*. [doi:10.1063/1.3273409]

I. INTRODUCTION

Magnetization reversal in magnetic thin films has been the focus of intensive research for several decades, because of the theoretical and practical importance to understand the hysteresis loops of thin films and multilayers.[1–9] When the magnetic hysteresis loop is measured for varying angle of the applied field, in-plane or out-of-plane of the film, the coercive field H_c is generally found to vary with the angle between the magnetic field direction and the easy axis of magnetization. Experimentally the magnetization reversal mechanism is usually inferred from this angular dependence of coercivity (ADC). Since the reversal mechanism is of great importance for switching and memory applications, there have been numerous investigations of ADC behaviors of various magnetic films.[10–16] Gau and Brucker[16] have studied the angular variation of coercivity of evaporated cobalt-based films. They observed that the angular variation of the coercivity curve exhibited different shapes, depending on the orientation of the easy axis, namely, a bell-shaped curve for an isotropic film, an M-shaped curve for a perpendicular deposited film, and a shifted M-shaped curve for an oblique deposited film with a tilted easy axis. The results of Huang and Judy[13] indicated that magnetization reversal in their rf sputtered Co–Cr perpendicular media followed a curling or buckling mode.

More recently, manganites, especially $La_{0.67}Sr_{0.33}MnO_3$ (LSMO) thin films, have raised considerable interest because of their special properties such as colossal magnetoresistance, high spin polarization of conduction electrons, and high Curie temperature (T_C=370 K). These properties may be of great advantage for the application in magnetic tunnel junction (MTJ) memory and sensing devices, using the switching or rotation of the magnetization direction in one electrode with respect to that in the other electrode. For such devices, the coercive fields and the reversal mechanism of the electrodes are important for the performance. The angular dependence of the coercivity in manganite thin films has hardly been studied, despite many works on the magnetic properties of LSMO magnetic thin films,[17–25] apart from the M-shaped angular dependence observed for a thin LSMO film on high vicinal angle $SrTiO_3$ (STO) showing strong uniaxial anisotropy reported by Wang *et al.*[18] Here, we report on the magnetization reversal mechanism, based on a detailed study of the ADC in LSMO thin films on $NdGaO_3$ (NGO) substrates with $(100)_o$ and $(110)_o$ surface orientation. (We will refer with subindex "o" to the orthorhombic lattice structure of NGO and with "pc" to the pseudocubic crystal structure of LSMO.) Such films experience anisotropic in-plane compressive strain, giving rise to a strong in-plane uniaxial magnetic anisotropy with different anisotropy strengths depending on the amount of strain, as determined by the substrate orientation.[25] It is shown that the strain differences are reflected in the ADC. The observed M-shaped ADCs are described by a two-phase model for the reversal.

II. REVERSAL MECHANISMS

In studies of magnetization reversal mechanism, one seeks to understand the character of the switching of a magnetic structure. There are various routes to reversal, depending on structure size, ranging from fast, deterministic, quasi-coherent rotation (CR) in submicron-size magnetic elements to slower, stochastic domain wall (DW) nucleation and propagation in larger thin films. For single domain magnets with a single anisotropy axis, in which the magnetization reversal process is governed by the collective rotation of the magnetic moments, the angular dependence of the coercive field H_c is described by the theory of CR of the magnetization vector according to the Stoner-Wohlfarth model.[4,26–28] For field angle θ, corresponding to the angle between the easy axis and the applied field direction, the coercive field coincides with the switching field $H_c^{CR}(0<\theta\leq 45°) = H_{sw}(\theta) = H_A(\cos^{2/3}\theta + \sin^{2/3}\theta)^{-3/2}$. In this range the magnetization loop (MH-loop) is infinitely steep at the coercive

[a]Author to whom correspondence should be addressed. Electronic mail: e.p.houwman@utwente.nl.

field. For $45° < \theta \leq 90°$ the hysteresis loop is sheared at $H_c^{CR}(45° < \theta \leq 90°) = (H_A/2)\sin 2\theta$ and switching occurs only after the magnetization changes sign. Here, H_A is the anisotropy field, $H_A = 2K_u/\mu_0 M_s$, with K_u the uniaxial anisotropy energy, and M_s the saturation magnetization. In the case of CR H_c is a monotonously decreasing function of θ. This mechanism generally applies to small particles only, since then divergence of the magnetic moments within the particle is energetically unfavorable because of the increase in the exchange energy.

For particle sizes larger than a certain critical size, magnetization reversal may occur by the curling mechanism.[1] This model was developed for an ellipsoid in which the magnetization switching occurs through a curling rotation of the magnetization around the easy axis, i.e., the long axis of the spheroid. In this way the increased exchange energy is less than the energy gain arising from a reduction in the demagnetization energy during this process. The magnetization switch is an abrupt process at the switching field; hence it is assumed that $H_c = H_{sw}$. However, the model configuration and assumptions are not well applicable to the thin films considered here, which have in-plane magnetization and large crystal anisotropy on top of the small in-plane shape anisotropy.

For uniaxial magnets in which the reversal mechanism is controlled by DW depinning, the coercivity is in its simplest form described by the Kondorsky[29] relation $H_c^{Kon}(\theta) = H_c(0)/\cos\theta$. Here, the physical picture is that the energy cost to displace a DW from a potential energy minimum is supplied by the difference in Zeeman energy of the states with opposite magnetizations. DWs start to move when the field surpasses a switching field, $H_{sw}^{Kon}(\theta) = H_{sw}^{Kon}(0)/\cos\theta$, initiating the reversal. If the DW motion is not stopped before complete reversal has taken place, one can identify the coercive field with the switching field $H_{sw}^{Kon}(\theta) = H_c^{Kon}(\theta)$, and the MH-loop is infinitely steep at the coercive field. In this expression the angular dependence has been separated from the material dependent factors, determining $H_c(0)$. Clearly this relation diverges at angles close to 90°. This is a consequence of the fact that it is assumed that the magnetization vector is not rotating away from the anisotropy axis, irrespective of the field angle and field strength. Although more sophisticated models take into account the field angle dependence of the DW energy,[5] thus removing the divergence of the Kondorsky relation, such models do not reproduce the M-shaped ADC observed for our films, as discussed below.

A different approach is followed by Grechiskin *et al.*[30] Here it is assumed that the magnetization curve is composed of single domain phase branches, described by the CR model and two-phase branches, described by Néel's phase theory.[31,32] Decreasing the applied field from saturation, the system follows the single domain branch. At a certain nucleation field, DWs nucleate in the material and the two-phase system arises. A DW moves freely through the sample and its equilibrium position is determined by the thermodynamic equilibrium of the two phases, which in turn is dependent on the applied field. Thus the field displaces the DW, but also rotates the magnetization vectors in the domains. This is possible when the anisotropy is not too strong as compared to shape anisotropy. When the DWs merge, the system is in the single domain phase again and follows the CR branch again. Note that for such a magnetization loop it is required that the DWs can move freely once they have been created. The resulting expression for the coercive field in such a two-phase system is[15,30]

$$H_c^{2-ph}(\theta) = H_c(0)\frac{(N_x + N_N)\cos\theta}{N_z \sin^2\theta + (N_x + N_N)\cos^2\theta}. \quad (1)$$

For $\theta = 0°$ the coercive field is equal to the nucleation field $H_c(0)$. N_z and N_x are the demagnetizing factors in the z-axis direction [corresponding to the (in-plane) easy axis direction of the thin films considered here] and x-axis direction, respectively. Both axes are in the plane of the magnetic field and of the magnetization rotation. We assume that for our samples the magnetization is predominantly in the plane of the film, because of the thin film demagnetization. $N_N = H_A/M_S$ is a formal parameter that can be interpreted as an effective demagnetizing factor due to the effect of an anisotropy mechanism other than shape anisotropy. For a large ratio $y = (N_x + N_N)/N_z$, implying a strong anisotropy as compared to shape anisotropy, the above equation reduces to the original Kondorsky relation. This equation predicts a maximum close to the hard axis direction and for single crystals $H_c^{2-ph}(90°) = 0$. Hence, the divergence in the hard axis direction is removed and replaced with a minimum. For polycrystalline materials, one expects an easy axis distribution, resulting in $H_c^{2-ph}(90°) \neq 0$.[30]

III. EPITAXIAL LSMO THIN FILMS ON NGO $(100)_o$ AND NGO $(110)_o$

Epitaxial LSMO thin films were grown on single terminated NGO substrates with $(100)_o$ and $(110)_o$ surface plane orientations, respectively.[25] Pulsed laser deposition from a stochiometric target in an oxygen background pressure of 0.35 mbar with a laser fluence of 3 J/cm^2 was used. The substrate temperature was 750 °C. The target to substrate distance was fixed at 4 cm. After LSMO deposition, the films were cooled to room temperature at a rate of 10 °C/min in a 1 bar oxygen atmosphere. The commonly used $NGO(110)_o$ substrate gives $(001)_{pc}$ pseudocubic growth of the LSMO film, whereas in the case of $NGO(100)_o$ the LSMO pseudocube grows 45° canted, i.e., in the $(011)_{pc}$ direction.[25]

Atomic force microscopy measurements show smooth surfaces with unit cell step height in accordance with the orientation of the surface, approximately 3.9 and 2.7 Å for the $(001)_{pc}$ and $(011)_{pc}$ oriented films, respectively. The latter step height corresponds to approximately half the height of the canted cube, 5.52 Å. In this case the film surface is expected to consist of either LaSrMnO- or pure O-planes.

X-ray diffraction (XRD) measurements were used to determine the directions of the crystal axes of the NGO substrate and the structure of the LSMO film. In Fig. 1 we show the reciprocal space maps of several reflections of a 20 nm LSMO film on a $NGO(100)_o$ film and of a 52 nm LSMO film on $NGO(110)_o$. All the maps show that the in-plane components of the film peaks are at the same position as those of the corresponding substrate peaks, whereas the out-of-plane

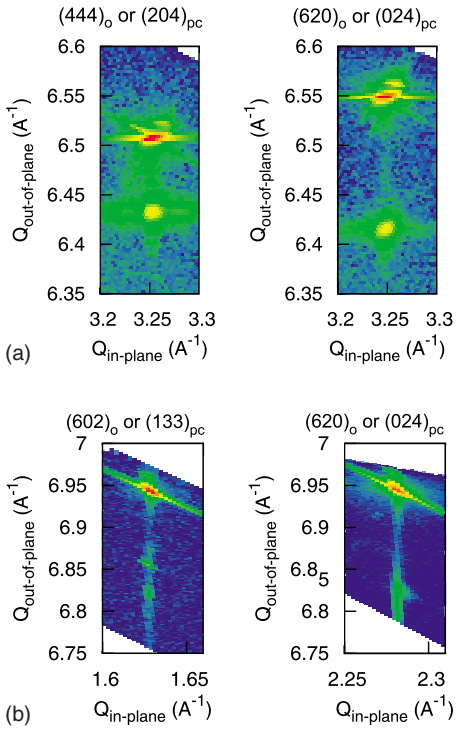

FIG. 1. (Color online) (a) Reciprocal space maps of the $(444)_o$ and $(620)_o$ XRD reflections of a 52 nm LSMO film on NGO$(110)_o$. In the pseudocubic notation these peaks correspond to the $(204)_{pc}$ and $(024)_{pc}$, respectively, for this film grown in the $(001)_{pc}$ direction. (b) Idem for $(602)_o$ $[(133)_{pc}]$ and $(620)_o$ $[(024)_{pc}]$ of a 20 nm LSMO film, grown in the $(011)_{pc}$ direction on NGO$(100)_o$.

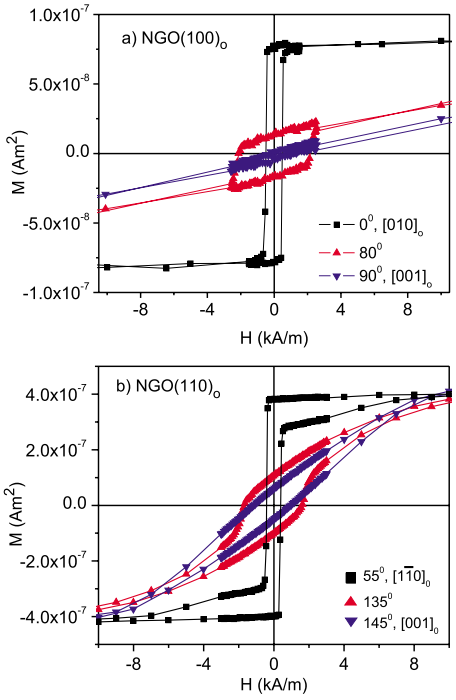

FIG. 2. (Color online) (a) Hysteresis loops of a 15 nm thick LSMO on NGO$(100)_o$ with the in-plane field applied in the 0° (NGO$[001]_o$ direction), and 80° and 90° (NGO$[010]_o$) at room temperature. The film surface steps are along the NGO$[010]_o$ direction. (b) Idem for a 52 nm LSMO on NGO$(110)_o$ measured at in-plane field angles 55° (NGO$[001]_o$), and 135° and 145° (NGO$[1\bar{1}0]_o$). The film surface steps are in the 90° direction.

peak positions are slightly different. This means that the lengths of the in-plane pseudocubic lattice vectors of the LSMO film correspond to the lengths of the in-plane substrate lattice vectors,[25] indicating coherent, epitaxial growth. The out-of-plane LSMO lattice vectors were determined as 3.906 and 5.51 Å for the NGO$(110)_o$ and NGO$(100)_o$ substrates, respectively. The second reflection of the 20 nm film at $Q_{out\text{-}of\text{-}plane}=6.86$ Å^{-1} is ascribed to a twin in the substrate. The satellite peaks in the thick film are due to anisotropic lattice modulations.[33]

Room temperature in-plane magnetic anisotropy measurements were performed using a vibrating sample magnetometer. For each film, hysteresis loops were taken at different in-plane field directions with intervals of 5°. Figure 2(a) shows three hysteresis loops obtained for a 15 nm thick LSMO film on NGO$(100)_o$, taken along 0°, 80°, and 90° with respect to one edge of the substrate in the NGO$[010]_o$ direction. The field directions 0° and 90° were found to be the in-plane easy and hard directions, respectively. The hysteresis loop taken at field angle $\theta=\theta_{max}=80°$, very close to the hard direction, shows the highest coercivity. Figure 2(b) shows the hysteresis loops obtained for a 52 nm thick LSMO film on NGO$(110)_o$, taken along 55°, 135°, and 145° with respect to one edge of the substrate direction. XRD analysis shows that 55° is in the in-plane crystal direction NGO$[1\bar{1}0]_o$ and 145° in the $[001]_o$ direction. The field directions 55° and 145° correspond to the in-plane easy and hard directions, respectively. Again close to the hard direction (135°) the highest coercivity is observed.

The remanent magnetization values, determined from the loops obtained from different films on NGO$(100)_o$ and $(110)_o$, are shown in Fig. 3. The experimental $M_r(\theta)$ dependencies show unambiguously the uniaxial $M_r(\theta)=M_s|\cos\theta|$ dependence, due to the projection of the easy axis magnetization onto the axis of observation. The coercive field dependencies in the same figure exhibit the M-type curve; i.e., with an increase in applied field angle, measured from the in-plane easy direction, the coercivity first increases, reaches a peak value, and then decreases sharply as the field direction approaches the in-plane hard axis. We observed the same qualitative $M_r(\theta)$ and $H_c(\theta)$ behaviors for all our LSMO films of different thicknesses and grown on NGO substrates with different orientations, NGO$(100)_o$ and NGO$(110)_o$, but also on NGO$(001)_o$ and NGO$(010)_o$ and (for thin LSMO films on) NGO$(112)_o$.[24,25]

IV. DISCUSSION

The experimental coercivity curves have been scaled with H_A, estimated from the hard axis magnetization loops. The uniaxial anisotropy constant is estimated from the magnetization loops as $K_u=5.7$ and 2.1 kJ/m^3 for the 9 nm thick LSMO film on NGO$(100)_o$ and the 52 nm film on NGO$(110)_o$ of Fig. 2, respectively. The difference is ascribed to the difference in substrate induced strain.[25] H_A is the scaling field for the CR model, and defines the maximum switching field. In Fig. 3 the theoretical angle dependence of the coercive field as calculated from the CR model is depicted (narrow V-shaped curve between the maxima and the zero's of H_c at the hard axis angles). The vertical axis extends over

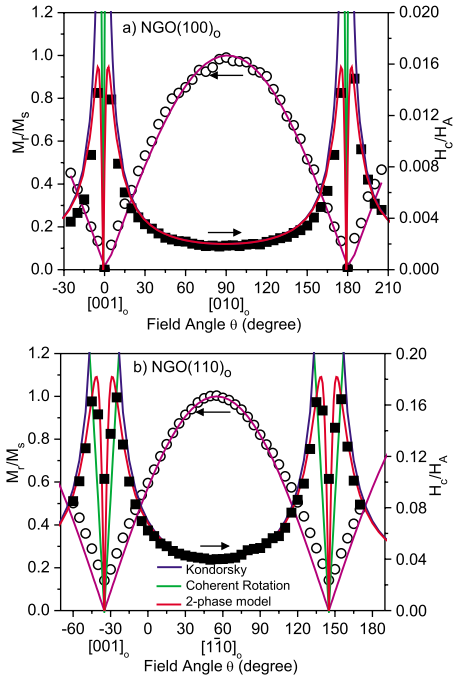

FIG. 3. (Color online) Remanence (■) and coercivity (○) vs in-plane field angle of (a) 9 nm thick LSMO/NGO(110)$_o$ and (b) 52 nm LSMO/NGO(110)$_o$ at room temperature. The remanence is fitted with $M_r = M_s|\cos\theta|$. Theoretical curves for the coercive field are according to the CR model (for angles between maxima and zero minimum in H_c), the Kondorsky model (between maxima and shallow non-zero minimum) and the two-phase domain-wall motion models (for all angles).

the low H_c/H_A values; therefore only the part of the H_c^{CR} curve close to the hard axis is visible (H_c^{CR}/H_A is equal to 1 for $\theta=0$). Furthermore, the data have been fitted according to the Kondorsky (U-shaped curve extending between the maxima and the broad local minimum at the easy axis angle) and the two-phase model (used for all angles), with experimentally determined values $H_c(\theta=0)=0.08$ kA/m for the 9 nm film on NGO(100)$_o$ and 0.40 kA/m for the 52 nm film on NGO(110)$_o$, respectively. This corresponds to $H_c(0)/H_A = 0.002$ and 0.04. From the fit with the two-phase model we obtain $y \approx 250$ and 82. From these values and knowing that for the square shaped thin film samples with in-plane magnetization, the in-plane demagnetization factors are approximately equal, $N_z = N_x = N$, one can obtain an estimate for N for each film, which is a function of the film thickness-side length ratio c/a.[34] From the known film thicknesses, we estimate $a \approx 230$ μm for both films. We interpret this macroscopic size as the average dimension of the film section that behaves according to the two-phase model. The experimental H_c data for the thin film [on NGO(100)$_o$] show a very sharp minimum in the magnetic hard direction, equal to H_c(hard) $=0$, indicating a negligible spread of the easy axis directions in the film, whereas the H_c data for the thick film [on NGO(110)$_o$] show the indication of a finite hard axis minimum. Although the latter may be due to a slight misalignment from the hard axis direction, it could also be an indication of some spread in the easy axis directions. This is supported by the $M_r(\theta)$ measurements, showing a finite minimum in the hard axis direction, which can easily be explained as being the result of the superposition of $|\cos\theta|$ dependencies with a narrow distribution of easy axis directions. Such a distribution may be attributed to strain relaxation with increasing film thickness, causing the easy axis to rotate slightly away from the substrate-strain induced uniaxial easy axis direction to that of relaxed LSMO. Theoretically the relative peak height $H_{c,\max}(\theta_{\max})/H_c(0)$ of the $H_c^{2-ph}(\theta)$ curve is equal to $y/2\sqrt{y-1}$ ($\approx\sqrt{y}/2$ for large y values). The different relative peak heights in Fig. 2 are a consequence of the factor of 6 difference in N_A and the factor of 2 difference in N of these films.

Close to the hard axis the H_c^{2-ph} curves nearly coincide with the H_c^{CR} curves. The HM-loops for field angles below the maximum in the H_c curve all show well discernible switching, at field values approximately equal to H_c. Note, however, that the switching is not sharp for $\theta=\theta_{\max}$. Instead the curves are sloped and the slopes increase with increasing field angle, finally to reach the slope of the hard axis curve of the CR model. This behavior is characteristic for the two-phase model and reflects the displacement of the DWs, shifting the ratio of the two phases and thus changing the net magnetization. This is in contrast with the Kondorsky model that assumes a vertical MH-loop at the switching field. In the Kondorsky model a sloped loop beyond the switching field may be interpreted as being due to a distribution of switching fields in the sample. We observe that for larger field angles the switching cannot be distinguished anymore and the curves become smooth, approximately like the CR loops at high field angles [but without showing the switching at field values larger than $H_c(\theta)$]. The initial increase in $H_c(\theta)$ and the rapid decrease beyond $\theta_{\max}$ have earlier been interpreted as a change from Kondorsky type reversal to CR-type reversal, in the case of a LSMO film on high vicinal angle STO showing strong unixial anisotropy.[17] Using the two-phase model it is not necessary to assume this crossover between switching mechanisms. This is because this model contains both DW motion, dominant at angles below $\theta_{\max}$, and the large rotation of the magnetization in the domains for angles close to the hard direction. We believe therefore that also in the case of Ref. 17 the two-phase model result gives a better interpretation of the observed loops and ADC behavior.

These results may be used to optimize the design and performance of MTJs based on manganite thin films, which can be described by the two-phase model. By choosing the applied field in the junction electrodes parallel to the in-plane magnetic easy axis, imposed by substrate induced strain, one expects to observe abrupt resistive switching of the junction when the electrode magnetization reverses direction. On the other hand, when there is an angle between the applied field and the easy axis direction, the net magnetic change goes more gradually in the switching field range of the MTJ. Also in the domains the magnetization rotates gradually. Depending on the number of domains under the tunnel barrier, the resistive switching becomes dependent on the position of the DW and the magnetization direction in the domains. This is expected to result in a more gradual change in resistance. Further the high resistance state is expected to show less resistance, because in this case the magnetization vectors in both electrodes make a less than optimal angle for maximum, i.e., less than 180°.

V. CONCLUSIONS

High-quality epitaxial LSMO thin films have been grown coherently on $NGO(100)_o$ and $NGO(110)_o$. The anisotropic in-plane strain gives rise to a strong uniaxial magnetic (in-plane) anisotropy. This is observed in the angular dependence of the remanence and coercivity. For both substrates the angular dependence of the coercivity shows a characteristic "M-shaped" curve. This dependence is well explained in terms of the two-phase model, giving a good quantitative agreement with the experimentally measured ADC curves.

ACKNOWLEDGMENTS

We acknowledge financial support from the NanoNed, the nanotechnology network in the Netherlands, the Dutch Technology Foundation (STW), the Netherlands Organization for Scientific Research (NWO), and the EU program Nanoxide.

[1] A. Aharoni, J. Appl. Phys. **82**, 1281 (1997).
[2] A. Moschel, R. A. Hyman, A. Zangwill, and M. D. Stiles, Phys. Rev. Lett. **77**, 3653 (1996).
[3] J. M. Florczak and E. Dan Dahlberg, Phys. Rev. B **44**, 9338 (1991).
[4] A. Aharoni, *Introduction to the Theory of Ferromagnetism*, 2nd ed. (Oxford University Press, New York, 2000).
[5] F. Schumacher, J. Appl. Phys. **70**, 3184 (1991).
[6] F. Cebollada, M. F. Rossignol, D. Givord, V. Villas-Boas, and J. M. González, Phys. Rev. B **52**, 13511 (1995).
[7] D. Zhao, L. Feng, D. L. Huber, and M. G. Lagally, J. Appl. Phys. **91**, 3150 (2002).
[8] R. Dittrich, G. Hu, T. Schrefl, T. Thomas, D. Suess, B. D. Terris, and J. Fidler, J. Appl. Phys. **97**, 10J705 (2005).
[9] P.-L. Lu and S. H. Charap, IEEE Trans. Magn. **28**, 986 (1992).
[10] C. Byun, J. Sivertsen, and J. Judy, IEEE Trans. Magn. **22**, 1155 (1986).
[11] Y.-N. Hsu, S. Jeong, D. E. Laughlin, and M. E. McHenry, IEEE Trans. Magn. **36**(5), 2336 (2000).
[12] J. J. Wyslocki, P. Pawlika, W. Kaszuwara, and M. Leonowicz, J. Magn. Magn. Mater. **242–245**, 1344 (2002).
[13] M. Huang and J. H. Judy, IEEE Trans. Magn. **27**, 5049 (1991).
[14] R. Ranjan, J. S. Gau, and N. Amin, J. Magn. Magn. Mater. **89**, 38 (1990).
[15] N. P. Suponev, R. M. Grechishkin, M. B. Lyakhova, and Y. E. Pushkar, J. Magn. Magn. Mater. **157–158**, 376 (1996).
[16] J. S. Gau and C. F. Brucker, J. Appl. Phys. **57**, 3988 (1985).
[17] K. Steenbeck and R. Hiergeist, Appl. Phys. Lett. **75**, 1778 (1999).
[18] Z. H. Wang, G. Cristiani, and H. U. Habermeier, Appl. Phys. Lett. **82**, 3731 (2003).
[19] P. Lecoeur, P. L. Trouilloud, G. Xiao, A. Gupta, G. Q. Gong, and X. W. Li, J. Appl. Phys. **82**, 3934 (1997).
[20] C. Kwon, M. C. Robson, K.-C. Kim, J. Y. Gu, S. E. Lofland, S. M. Bhagat, Z. Trajanovic, M. Rajeswari, T. Venkatesan, A. R. Kratz, and R. Ramesh, J. Magn. Magn. Mater. **172**, 229 (1997).
[21] J. Dho, Y. N. Kwo, Y. S. Hwang, J. C. Kim, and N. H. Hur, Appl. Phys. Lett. **82**, 1434 (2003).
[22] F. Tsui, M. C. Smoak, T. K. Nath, and C. B. Eom, Appl. Phys. Lett. **76**, 2421 (2000).
[23] M. Mathews, F. M. Postma, J. C. Lodder, R. Jansen, G. Rijnders, and D. H. A. Blank, Appl. Phys. Lett. **87**, 242507 (2005).
[24] H. Nishikawa, E. P. Houwman, J. A. Boschker, M. Mathews, G. Rijnders, and D. H. A. Blank, Appl. Phys. Lett. **94**, 042502 (2009).
[25] J. A. Boschker, M. Mathews, E. P. Houwman, H. Nishikawa, A. Vailionis, G. Rijnders, and D. H. A. Blank, Phys. Rev. B **79**, 214425 (2009).
[26] E. C. Stoner and E. P. Wohlfarth, Philos. Trans. R. Soc. London, Ser. A **240**, 599 (1948); IEEE Trans. Magn. **27**, 3475 (1991).
[27] S. Chikazumi and C. D. Graham, *Physics of Ferromagnetism*, 2nd ed. (Oxford University Press, Oxford, 1997).
[28] L. Sun, Y. Hao, C.-L. Chien, and P. C. Searson, IBM J. Res. Dev. **49**, 79 (2005).
[29] E. Kondorsky, J. Phys. (USSR) **2**, 161 (1940).
[30] R. M. Grechishkin, S. S. Soshin, and S. E. Ilyashenko, First International Workshop on Simulation of Magnetization Processes, SMP'95, Vienna, Austria, 1995 (unpublished), p. 72.
[31] M. L. Néel, J. Phys. Radium **11**, 18 (1944).
[32] M. L. Néel, J. Appl. Phys. **31**, S27 (1960).
[33] A. Vailionis, J. A. Boschker, E. P. Houwman, G. Koster, G. Rijnders, and D. H. A. Blank, Appl. Phys. Lett. **95**, 152508 (2009) (note that in this reference LSMO is described in the orthorhombic lattice system, whereas in the present paper the pseudocubic notation is used).
[34] A. Aharoni, J. Appl. Phys. **83**, 3432 (1998).